Multiple excitation fluorometer for *in situ* oceanographic applications

Russell A. Desiderio, Casey Moore, Carl Lantz, and Timothy J. Cowles

A new *in situ* fluorometer for the detection of oceanic photosynthetic pigment fluorescence is described. Emission spectra from 546 to 733 nm are recorded for each of three different visible excitation bands ten times a second. A Spectralon cell is used to improve the excitation coupling to and the collection efficiency from the sample volume. Laboratory tests demonstrated that the fluorescence emission spectra from the violet, blue, and green excitation can be used to discriminate among various algal species. The instrument was used at sea in extended *in situ* deployments on an undulating vehicle (SeaSoar).

Key words: *In situ* excitation fluorometer, chlorophyll fluorescence, oceanography.

1. Introduction

Chlorophyll fluorescence is used routinely as an indicator of phytoplankton biomass in marine and freshwater habitats. To date most of the commercially available *in situ* chlorophyll fluorometers have used broadband excitation and collection as a means to enhance sensitivity so that typical oceanic concentrations of chlorophyll could be detected.[1–3]

The photosynthetic apparatus of plants includes additional accessory pigments (such as carotenoids and phycobilins) that absorb light of wavelengths outside the chlorophyll absorption band and channel a portion of this excitation into the photosynthetic pathway.[4,5] With the exception of phycobilin pigments such as phycoerythrin most of these accessory pigments do not exhibit *in vivo* fluorescence. The occurrence of the accessory pigments and thus the extent to which chlorophyll fluoresces are dependent on the algal species and the environmental conditions experienced by that species. Therefore information on the taxonomic composition of the phytoplankton and of their physiological state is contained in the fluorescence excitation and emission spectra.[6,7]

We have designed and built an *in situ* fluorometer to monitor emission spectra from 546 to 733 nm as a function of three excitation wavelength bands in the visible. This design contrasts with other fluorometers that could incorporate variable excitation wavelengths if one were to change manually the excitation filter inside the instrument after each cast.[8,9]

2. Instrument Design

A. Optical

A schematic of the fluorometer is shown in Fig. 1. A 28-W quartz-tungsten-halogen lamp with an approximate color temperature of 3050 K was chosen to be the source because these lamps are inexpensive and relatively efficient. The lamp is mounted within an approximately parabolic dichroic reflector to reflect visible photons selectively down the optic axis. The broadband output is filtered further by IR-absorbing tempered KG3 Schott glass, whereupon it is focused by an antireflection MgF_2-coated aspheric lens so that the focal spot is approximately 10 mm in diameter. A filter wheel containing three interference filters (each 25.4 mm in diameter) is situated so that the focal spot sequentially illuminates each interference filter as the wheel rotates. A small right-angle prism is positioned to reflect a portion of the filtered light into a reference detector to monitor lamp-intensity changes as a function of wavelength and time.

Two antireflection-coated aspheric lenses are used as relay lenses to focus the excitation energy through a pressure window to the sample volume, which is enclosed in a removable 50-mm-long Spectralon cell

R. A. Desiderio and T. J. Cowles are with the College of Oceanic and Atmospheric Sciences, Oregon State University, 104 Oceanography Administration Building, Corvallis, Oregon 97331-5503. C. Moore and C. Lantz are with WETLabs, Inc., P.O. Box 518, Philomath, Oregon 97370.

Received 31 January 1996; revised manuscript received 15 July 1996.

0003-6935/97/061289-08$10.00/0

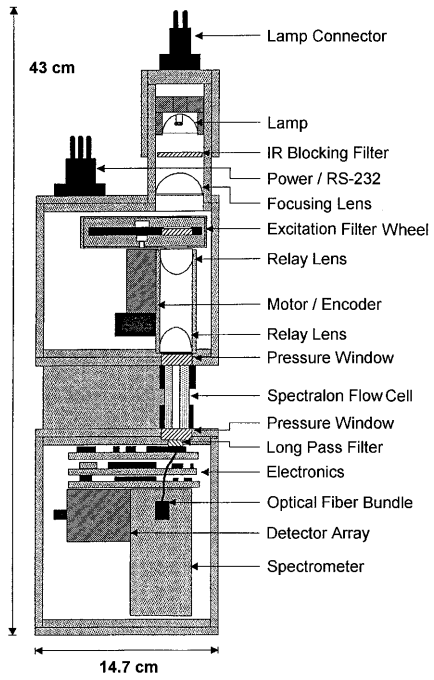

Fig. 1. Fluorometer schematic.

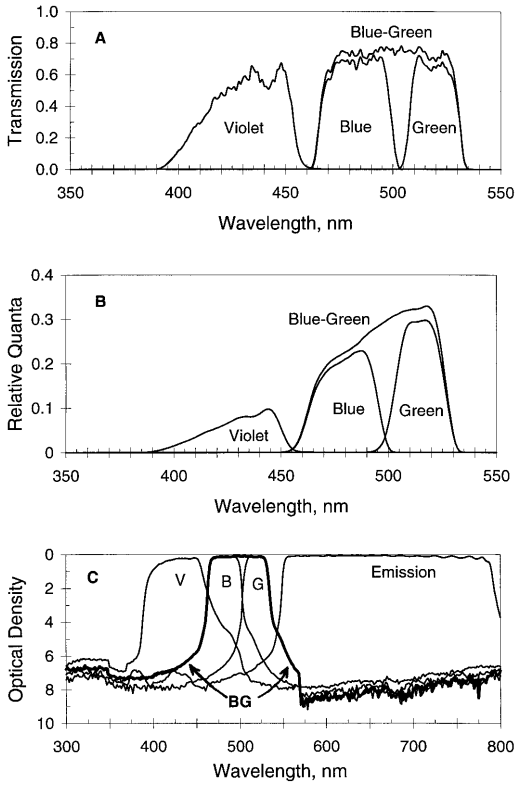

Fig. 2. A, Transmission of excitation filters. Spectra were measured at normal incidence on a Cary 3E spectrophotometer. B, Relative excitation intensity in sample volume. Note the influence of the spectral dependence of the lamp output. C, Optical density of interference filters. Spectra were measured at normal incidence on a Cary 3E spectrophotometer with neutral density filters in the reference beam and with the sample compartment covered with black cloth. This extends the sensitivity of this instrument to approximately an optical density of 7 at 800 nm and optical density 8 in the visible, as determined with a set of neutral density filters. The blocking of the blue-green broadband filter (dark trace) is the same as that of the blue filter at wavelengths shorter than 500 nm and is the same as that of the green filter at wavelengths longer than 500 nm.

with an inside bore of 6.4 mm. (Spectralon is a proprietary, highly diffuse reflectance material available from Labsphere, Inc.) Flow ports are provided at both ends of the cell at right angles to the optic axis. The inside wall of the Spectralon cell diffusely reflects both those incident excitation photons that are not absorbed and any emission photons incident upon it. Benchtop experiments showed a fluorescence signal enhancement of approximately 1 order of magnitude with this 50-mm-long Spectralon cell versus a 50-mm-path-length glass cell; also, a factor of ~5 enhancement was realized with a 50-mm Spectralon path-length cell versus a 25-mm Spectralon path-length cell.

At the distal end of the cell is the pressure window interface to the emission module. A 550-nm longpass interference filter, fabricated without absorptive colored glass, is situated immediately against the pressure window; in contact with it is the spot end of a spot-to-slit fiber-optic bundle composed of ~70 200-μm silica core fibers (Polymicro FHP200220240). These fibers are arrayed into a 1-mm × 4-mm rectangle at the slit end, which is situated at the entrance to the spectrograph. The Instruments, SA SC-90 *f*2.5 spectrograph was custom modified by the manufacturer for extended wavelength coverage in the red by removing the entrance folding mirror and drilling a hole into the spectrograph casing so that the fiber bundle directly illuminates the 1150-groove/mm holographic grating at the appropriate angle of incidence to provide the required emission coverage. The American Holographic DA-38 detector is composed of a hybrid amplified Hamamatsu 4112 diode array. We used 20 of the 38 available 4.4-mm-high detector pixels, that are pitched on 1.0-mm centers. This results in a wavelength coverage of from 546 to 733 nm (average dispersion 9.35 nm/mm). The center wavelength of the first (bluest) pixel is at 550 nm, so that emission signals recorded from it will be low relative to those from the other pixels because of the transmission characteristics of the 550-nm longpass interference filter mentioned above.

Four excitation filters were custom fabricated for this application by Chroma Technology Corporation. The passbands of the violet, blue, and green excitation interference filters (Fig. 2A) were chosen to maximize the differences in pigment fluorescence intensity excited by these three excitation channels as a function of the presence of the different accessory pigments found in phytoplankton. In addition, a broadband blue-green excitation filter passband was specified to maximize accessory pigment excitation (in contrast with the violet channel that maximizes the excitation of chlorophyll). Because the incandescent source emits more light at the longer visible

wavelengths, the broadband blue–green excitation channel usually results in greater sensitivity in the detection of phytoplankton fluorescence.

One can estimate the number of excitation quanta as a function of wavelength transmitted into the sample volume by modeling the spectral dependencies of the lamp output, the reflection of the lamp's dichroic reflector, the transmission of the IR blocking filter, and the blue shift and broadening of the interference filter passband transmission in a converging light application (Fig. 2B). The effect of the spectral dependence of the lamp emission, which has an emission maximum at ~1000 nm, is clearly evident. Measurements of the excitation power exiting the transmitter-case pressure window are taken through a 6.4-mm aperture (to match the sample cell bore) mounted on the detector head of a power meter. The spectral modeling results are used together with the known wavelength dependence of the power meter responsivity to determine the spectrally integrated excitation channel powers and excitation quanta ratios. Typical excitation powers are: green, 6.1 mW; blue-green, 15.2 mW; blue, 6.5 mW; and violet, 3.0 mW, corresponding to the following excitation-quanta ratios: (2.4 : 5.7 : 2.4 : 1.0) :: (G : BG : B : V).

The out-of-passband blocking of the excitation and emission filters (Fig. 2C) is particularly important in fluorescence applications with broadband excitation sources, especially when a collinear optical geometry is used. The excitation filters were specified to have an optical density of 9 in the fluorescence emission region because the incandescent light source emits many more photons in this region than in the excitation region. The emission filter was specified to have an optical density of 6 in the excitation region. The optical density traces of these filters at their blocking regions show the spectrophotometer to be at its detection limit.

B. Electrical

The architecture of the electrical system is shown in Fig. 3. The motor controller for the filter wheel is controlled by the microprocessor to keep the rate of rotation at 10 Hz. A shaft encoder is used as a position sensor for the filter wheel and allows the microprocessor to remain synchronized with the angular position of the filter wheel.

The emitted light is detected with the DA-38 array that provides 20 emission channels of amplified electrical output to a channel-analog-multiplexer circuit. The channel-analog-multiplexer circuit is controlled by hardware in the digital serial interface in the microcontroller by way of a multiplexer digital sequencer. This guarantees that the microprocessor firmware that was used to collect the digitized channel data is always synchronized with the appropriate channel-analog signal. The 20 channels of spectrometer data and the reference detector circuit signal are multiplexed into two analog outputs.

The two outputs of the channel-analog-multiplexer circuit are fed into the channel-analog amplifier and level-shifter circuit. This processes the signals so

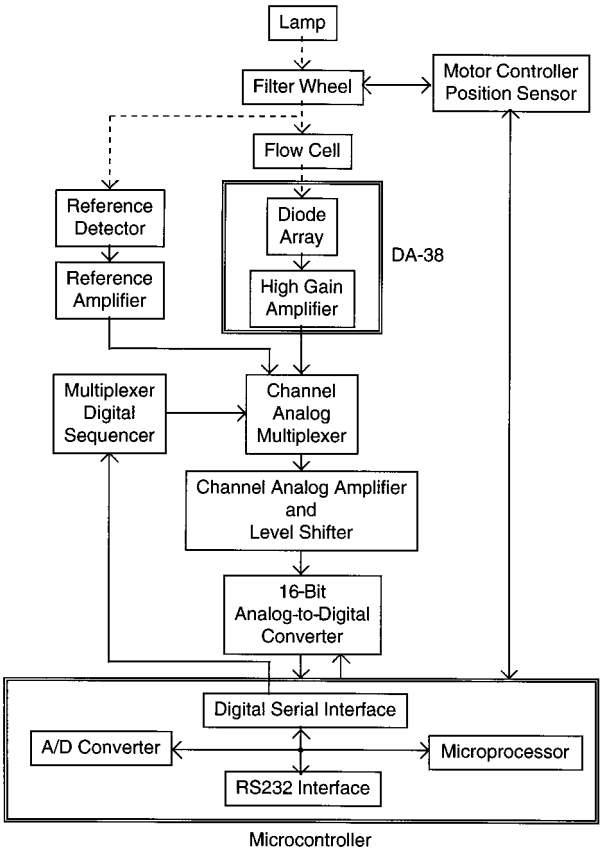

Fig. 3. Electrical block diagram. The dashed lines indicate light path.

that they are properly interfaced to the analog-to-digital converter (ADC). This circuit has a fast transient response time to ensure that switching between channels in the channel-analog multiplexer occurs fast enough to meet the setup time requirements of the ADC.

The ADC produces one 16-bit digital output for each of the two analog inputs. The analog-to-digital conversion occurs simultaneously for each analog input and is internally pipelined so that one analog-to-digital conversion is allowed to proceed while the subsequent analog signal is multiplexed and amplified. This overlapping of signal processing allows a continuous conversion rate of 150K conversions/s. The digital output of the ADC has a serial format. This connects to a digital serial interface module inside the microcontroller, where microprocessor firmware collects the digital data. The firmware processes the data and transmits them out of the instrument by an RS-232 interface. This operates at 38.4 Kbaud. The data are in a hexadecimal format, with a net transfer rate of 1730 bytes/s. A Request to Send signal is used as an RS-232 input to control the flow of data out of the instrument.

C. Operation

Data acquisition is synchronized to the rotational position of the filter wheel. The position sensor on the

filter wheel detects an index position, as well as a rotational displacement. Throughout the data-acquisition process the firmware is always synchronized to the filter wheel rotation to ensure that only valid data are processed.

The microprocessor firmware that controls the data acquisition waits for the index location, initializes its internal data structures, and builds the data packet header. The firmware then waits until the lamp shines through the first filter, at which time the fluorescence data are collected from the spectrograph. Each of the spectrograph channels is sampled in a round-robin sequence in the following manner: The spectroscopic signals are processed two at a time, one in each of the analog multiplexer circuits, until the first ten spectroscopic channels have been sampled by one of the multiplexer circuits and the second ten channels sampled by the other. The reference detector signals are sampled. Then, the entire sequence is repeated until each channel has been sampled 30 times. This sampling sequence allows uniform averaging of the spectroscopic data across the entire filter, so that 30 measurements for each emission pixel are obtained during each illumination of an excitation filter. Data are collected only while the entire lamp beam shines through the filter. Because the data have been oversampled, the average data value is then calculated for each of the spectrograph channels.

When the filter wheel has rotated so that all excitation light is blocked, the firmware takes an average reading for each of the spectrograph and reference channels in the manner described above. This background average value for each channel is then subtracted from the previously determined average data value for each channel to eliminate long-term signal drift. The resultant values are placed into an RS-232 transmit data buffer and are transmitted out of the instrument by firmware in a background mode.

This emission channel sampling process is then repeated for each of the other two excitation filters. The firmware then calculates the checksum for the data packet, builds the data packet footer, and places these data into the RS-232 transmit data buffer. Each data packet of 173 bytes consists of three fluorescence spectra, one for each excitation channel.

After all the data have been processed for one filter wheel revolution, the firmware waits for the index location and then repeats the entire process.

The instrument requires 28 W at 12 V to power the lamp; the rest of the electronics requires 3 W.

3. Instrument Characterization

We characterized instrument performance by analyzing emission spectra from chlorophyll *a* and cultures of four different species of algae.

A. Materials and Methods

Pure chlorophyll a, free from chlorophyll b, was obtained from Sigma (C-6144) and used without further purification. Concentrations of chlorophyll standards were determined from absorption measurements on a Cary spectrophotometer.

The *Dunaliella tertiolecta* cultures were grown in half-strength Institute for Marine Research media at 16 °C on a 14:10-h light:dark cycle. The *Cryptomonas profunda*, *Dunaliella salina*, and *Nitzschia costatum* cultures were grown in $F/2$ media on a 12:12-h light:dark cycle at a growth irradiance of between 300 and 500 μE. Filtered seawater (0.2 μm) was used as the solvent in culture dilution series. Unless otherwise noted, the chlorophyll concentrations of cultures were determined by baseline-corrected blank-subtracted absorption measurements at 676 nm with an ac-9 absorption and scattering meter (WETLabs) and by dividing by the conversion factor $a^*(676\ \text{nm}) = 0.017\ \text{m}^{-1}/(\mu\text{g chlorophyll/L})$ (where a* is the chlorophyll-specific phytoplankton absorption coefficient).

B. Results

The major source of the instrumental variability of the emission signal originates from the electronic noise arising from the DA-38 diode array and its amplifier. When spectra are accumulated with the entrance to the emission module blocked, each spectrographic channel shows a Gaussian variability in signal about a mean of zero characterized by a standard deviation of 19 counts, regardless of whether the lamp is on or off. However, virtually all the reference detector values are between ±2 counts (when the lamp is off). The spectroscopic channel outputs of the DA-38 and of the reference detector–amplifier channel outputs both feed into the same multiplexer (Fig. 3), so that the signal processing thereafter is the same for both. The electronic noise on the signal channels does decrease slightly as the instrument operating temperature decreases; a decrease in temperature of 10 °C results in a decrease of the standard deviation of the signal variability by 1 count.

The Raman peaks that are due to the symmetric stretch of the water molecule are easily detected in the emission spectra of water taken with green and blue excitation (Fig. 4). The corresponding Raman emission from the violet excitation is centered at ~510 nm and is therefore not present in that spectrum. When water is removed from the sample volume, the relatively strong broad peaks in the blue (emission at about 580 nm) and green (emission at about 620 nm) excitation spectra disappear. A weak broad peak, which is presumably due to either impurities or interference filter leakage, is evident in the chlorophyll emission region. This signal and the water Raman signal are removed when blank subtraction is used. The distribution of signal values in each channel was Gaussian with a mean standard deviation of 19, indicating that this variability in signal is due to the electronic noise of the instrument. Therefore the 95% confidence limits for the mean of each data point (determined from 1780 spectra) are given by ±2 standard errors ($\pm 2 * 19/\sqrt{1780} = \pm 1$ count) from the mean.

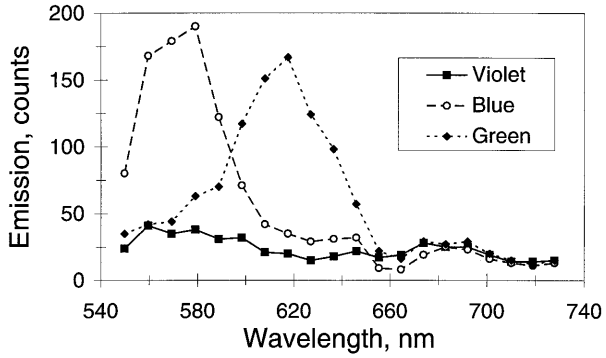

Fig. 4. Water emission spectra: violet, blue, and green excitation. Each spectrum was obtained by averaging 1780 spectra. Error bars representing the 95%-confidence limits (±2 standard errors from the mean) of these measurements lie within the data point character. Water was filtered, distilled, and purified by reverse osmosis. Spectra have not been corrected for the difference in the number of excitation quanta in each excitation channel.

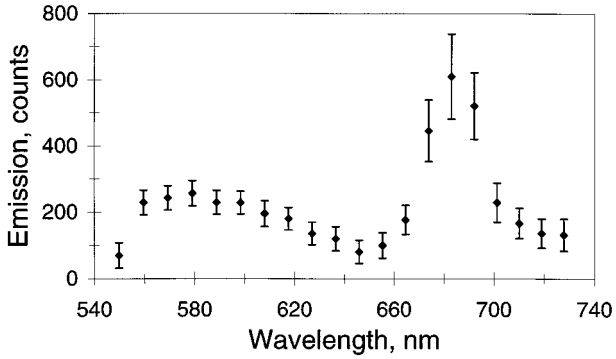

Fig. 6. Emission spectrum (broadband blue-green excitation) for a *Dunaliella tertiolecta* culture at a chlorophyll concentration of 1.2 μg/L. Each data point represents the mean of 120 separate spectra accumulated over 12 s; the error bars denote ±2 standard deviations for these 120 measurements.

The fluorescence response from extracted chlorophyll is linear for the green, blue, and blue-green excitation channels for concentrations of as much as 80 μg/L. For violet excitation, a negative deviation from linearity becomes noticeable at concentrations of 80 μg/L (Fig. 5). This could be expected to occur for at least two reasons. The more significant consideration is that the chlorophyll solutions absorb much more strongly in the violet than in the blue or the green; the linearity of a fluorescence response as a function of concentration is dependent on the approximation that the number of photons absorbed is linear with concentration, which is valid only for optically dilute solutions. A second consideration is that a negative deviation from linearity is also expected owing to the interaction of polychromatic excitation radiation on a sharply varying absorption line shape.[10] In any case, the data show that the response is still linear at a fluorescence peak intensity of 12,000 counts, indicating that at this signal level the detector and signal-processing electronics do not distort the response.

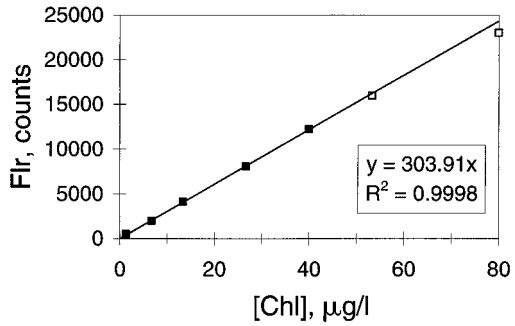

Fig. 5. Fluorescence (Flr) response (violet excitation) as a function of extracted chlorophyll (Chl) concentration. Peak fluorescence values are derived from blank-corrected averaged spectra. Error bars representing the 95% confidence limits (±2 standard errors from the mean) of these measurements lie within the data point character. The linear fit to the data is constrained to include the origin and excludes the data points at the two highest concentrations.

Different cultures of phytoplankton were used to evaluate instrument response to particulate matter containing different combinations of chlorophyll and accessory pigments. In all such cases the magnitude of chlorophyll fluorescence from cultures was a function of illumination time, in contrast to dispersed chlorophyll. Typically, the chlorophyll fluorescence from cultures showed a maximum after initial illumination, followed by a relatively fast decrease in signal of ~15% during the first second of illumination, followed by a slower decrease in signal thereafter. The time decay of the culture fluorescence intensity is not due to a corresponding decrease in excitation intensity, which is constant after the lamp is turned on. The signal from the Raman scattering of water is also constant as a function of time. The fluorescence measurements from cultures presented here were collected from static samples; only spectra after the initial rapid decrease in fluorescence signal ended were processed. Because the means of such fluorescence measurements depend on which spectra are selected to be averaged, spectral time series representing a given dilution series were analyzed identically with respect to the number of spectra averaged and the determination of the first spectrum to be processed relative to the time at which the lamp was turned on.

In the series of experiments carried out to determine the instrument detection limits the blue excitation filter was replaced by the blue-green excitation filter because its use generally results in the lowest detection limit for cultures owing to the spectral dependence of the incandescent source. Figure 6 represents 120 spectra with blue-green excitation taken of a culture of *Dunaliella tertiolecta* diluted to a concentration of 1.2 μg/L; the mean counts for each emission channel are shown, along with error bars representing ±2 standard deviations. The peak at 580 nm is due to Raman scattering from water and is broad because the blue-green excitation passband is broad. All the channels at wavelengths shorter than

650 nm show the same signal variability that is due to electronic noise as when spectra are accumulated with the emission module blocked. The signals in the chlorophyll fluorescence channels (at wavelengths longer than 650 nm) show a greater variability owing to the time dependence of the fluorescence signal; for the spectra analyzed here, the range of this variability is typically ~25% of the mean signal. When the magnitude of the variability of this time dependence is greater than or comparable to the variability owing to electronic noise, the spectral values in an emission channel are not normally distributed. The number that represents the standard error of the values in such a channel (standard deviation divided by the square root of the number of values) is an overestimate of the confidence limit of the channel's mean value. (If the time dependence of the signal were to be exactly linear, the mean would be determined exactly; but the standard deviation of the constituent values would still be nonzero). When the particulate chlorophyll concentrations are relatively low, the magnitude of the time-dependent decrease in fluorescence signal becomes much less than the variability owing to the electronic noise, so that then all the variability of the signals in all the channels is due to electronic noise. Under these conditions, the signal-to-noise ratio increases as the square root of the number of spectra averaged.

The definition of detection limit that we used in this study is that concentration of analyte that would result in a mean signal 2 standard errors above the blank baseline, which corresponds to a 97.7% (single-tailed) confidence limit.[10] Since the variability in the blank and analyte signals at the detection limit can be described by identical normal distributions, the one-spectrum detection limit is then given by the analyte concentration, resulting in a signal of $2\sqrt{2}$ standard deviations of the blank.

The detection limit can be lowered by averaging. The determination of the detection limit requires evaluation of measurements on a dilution series, including solutions of concentration at and less than the supposed detection limit (Fig. 7). In all excitation cases there is a linear relation between blank-subtracted fluorescence values and chlorophyll down to the detection limits. When the number of spectra N comprising both the blank and analyte averages is equal, the detection limits DL can be calculated (Table 1) as a function of $\sqrt{N}$, the standard deviation of the blank signal σ_{bl}, and the slope S of the linear regressions according to $DL = (2\sqrt{2}\sigma_{bl})/(S\sqrt{N})$. Because the excitation filter set used in these experiments consisted of the violet, blue-green, and green filters, the detection limits for blue excitation for this culture were estimated on the basis of experiments not presented here. The detection limits are always functions of the physiological state of the phytoplankton and are dependent on the particular suites of accessory pigments in the algal species used.

The fluorescence response of a culture of *D. tertiolecta* becomes noticeably nonlinear at a chlorophyll concentration of ~10 μg/L. The relative magnitude

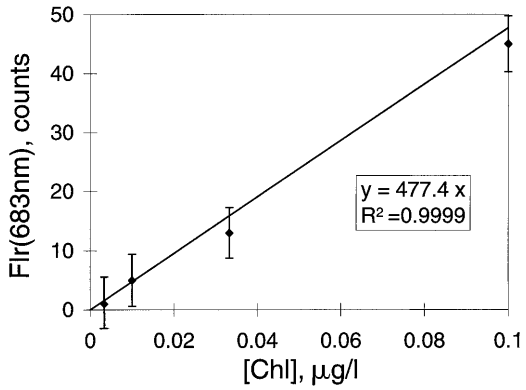

Fig. 7. Blank-subtracted fluorescence (Flr) intensities at 683 nm for blue-green excitation from a culture of *Dunaliella tertiolecta* as a function of chlorophyll (Chl) concentration. An averaged (179 spectra) distilled-water blank was subtracted from the average of 120 emission spectra to obtain the data values shown; error bars represent ±2 standard errors ε_{diff} about the difference of the means $[(\varepsilon_{diff})^2 = (\sigma_{flr})^2/120 + (\sigma_{wtr})^2/179]$. The linear fit includes data points at 0.3 and 1.2 μg/L, not shown, and is constrained to include the origin.

of the nonlinearity is greater for violet versus green excitation; and chlorophyll emission at wavelengths longer than that of the peak emission shows a more nearly linear response than does the chlorophyll emission at the emission peak. This behavior is typical of the response expected from an optically dense solution, as noted above in the discussion of the fluorescence response from extracted chlorophyll. (The red absorption peak of chlorophyll spectrally overlaps its fluorescence, so that there is more reabsorption of emitted photons at the wavelength of the emission peak than at longer wavelengths.) Furthermore, the relative deviation from a linear response is much less at a larger chlorophyll concentration (80 μg/L) for violet excitation of extracted chlorophyll (Fig. 5) at 23,000 counts (5.5%, assuming that the electronic response is linear in this region) than that for *D. tertiolecta* (violet excitation, 683-nm emission) at 27 μg/L and 3610 counts (21%). This is strong evidence for assigning the nonlinear fluorescence response of the cultures to the package effect,[11] in which

Table 1. Detection Limits (μg/L) as a Function of Number of Spectra Averaged N and Excitation Passband for a Culture of *Dunaliella tertiolecta*.

Number of spectra[a]	Violet	Blue[b]	Blue-Green	Green
N = 1	0.4	0.2 (est)	0.1	0.8
N = 10	0.1	0.06 (est)	0.04	0.2
N = 100	0.04	0.02 (est)	0.01	0.08

[a]Because the triplets of spectra are accumulated at a rate of 10 Hz, data acquisition times are 0.1, 1, and 10 s for N = 1, 10, and 100, respectively.

[b]The values for blue excitation are estimates (est) from the comparison of the violet fluorescence excitation results for *D. tertiolecta* with violet and blue fluorescence excitation results for *D. salina* in which the blue excitation filter was used in place of the blue-green filter.

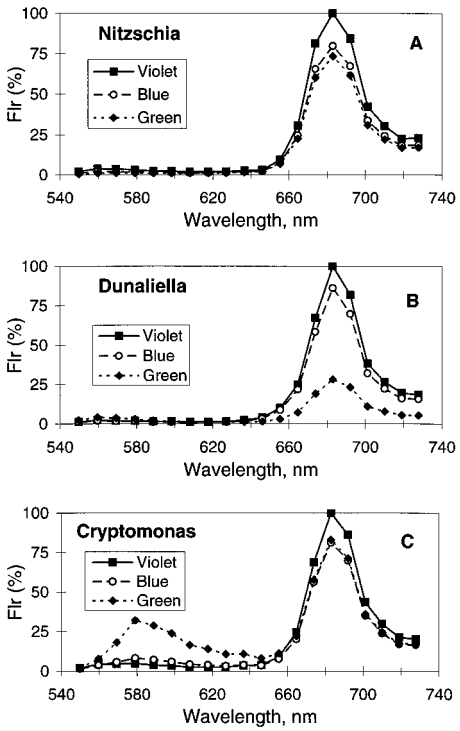

Fig. 8. Emission spectra from *Cryptomonas profunda, Nitzschia costatum*, and *Dunaliella salina* cultures; the extracted chlorophyll concentrations were determined by standard Turner fluorometric procedures to be 6, 9, and 14 μg/L, respectively. Fluorescence (Flr) values were derived from blank-corrected averaged spectra as detailed previously, then corrected for excitation channel intensity, and scaled to the fluorescence maximum in the respective violet channels.

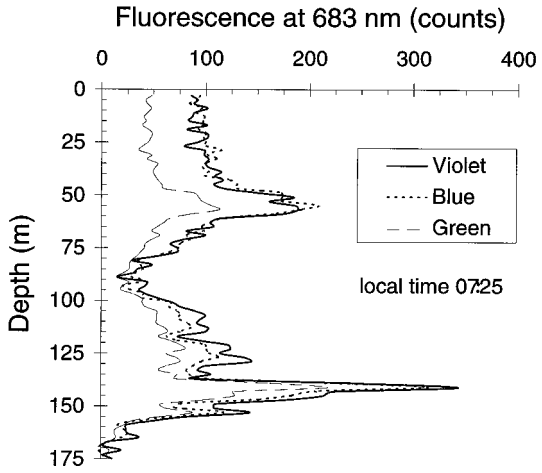

Fig. 9. Vertical profiles of photosynthetic pigment fluorescence (683-nm emission; violet, blue, and green excitation) in the California Current System in June 1993 from a SeaSoar hydrographic section at 37.87 °N. and 126.02 °W at 07:25-h local time. In this field study the blue excitation filter was replaced with the broadband blue-green excitation filter to maximize sensitivity. Fluorescence values for the blue excitation channel not present can be modeled by subtracting 1.12 times the green excitation channel fluorescence values from those of the blue-green channel [see Fig. 2(b)].

the cell packaging of chromophores serves to increase the optical nonlinearity of the system relative to the case in which the chromophores are uniformly dispersed throughout the sample volume.

Different classes of phytoplankton have different suites of photosynthetic accessory pigments, which in turn result in fluorescence efficiencies that vary as a function of excitation wavelength (Fig. 8). The fluorescence values in each excitation channel have been normalized to the corresponding total number of excitation channel quanta. In addition, each culture's fluorescence values are also scaled to result in a value of 100 at the red fluorescence peak in that culture's violet excitation channel. This scaling shows that the behavior of chlorophyll fluorescence excited by the blue channel relative to that excited by the violet channel is similar for these three particular cultures (for this reason the blue filter was the one replaced when the broadband blue-green filter was inserted to maximize instrument sensitivity). However, *Dunaliella salina* can be distinguished by its relatively low chlorophyll fluorescence when excited in the green; and the phycoerythrin fluorescence at 580 nm in the *Cryptomonas profunda* spectra differentiates it from the other two cultures.

We used this new instrument during cruises in June–July 1993 and August–September 1993 in the California Current System. We deployed the multiexcitation spectral fluorometer on an undulating towed instrumentation package (SeaSoar), which also carried a CTD (conductivity, temperature, depth) for characterization of the hydrographic conditions within the survey area. We can illustrate the variation in chlorophyll fluorescence intensity as a function of excitation at one position in this region by plotting the photosynthetic pigment fluorescence emission at 683 nm as a function of depth (Fig. 9). In the euphotic zone (above 55 m) the intensities of the violet- and blue-excited chlorophyll fluorescence are approximately the same and are approximately a factor of 2 higher than that excited by green light, whereas below 100 m the intensity of the blue-excited fluorescence is clearly lower that of the violet, which is still approximately a factor of 2 greater than that excited by green light. These differences in fluorescence emission indicate that the sampled water had different absorption spectra or different fluorescence quantum yields as a function of excitation wavelength. Detailed day–night comparisons among similar water types will help resolve whether these differences can be ascribed to accessory pigment composition or photoadaptive condition.

4. Discussion

The major advantages of the forward-scatter fluorescence geometry over a (more traditional) 90° geometry are a larger sample volume and perfect overlap and alignment of the excitation and collection fields. Implementation of the chosen geometry increases sensitivity and reduces analyte flicker noise (signal fluctuations due to encounter statistics of analyte

particles).[10,12] The disadvantage of the forward-scatter geometry is that a sublinear fluorescence response becomes apparent at relatively lower chlorophyll concentrations because, owing to the longer path length, optical nonlinearity is increased. This increased optical nonlinearity arises because the relatively greater number of photons absorbed is more nonlinear with concentration, and fluoresced photons have a greater probability of being (re)absorbed. The use of Spectralon as the sample cell material serves to increase both the sensitivity and the deviations from linearity because excitation and emission photons directed at the cell walls are diffusely reflected back into the sample volume. Because the detection limit (one shot) for particulate chlorophyll is 0.1 μg/L and deviations from linearity become apparent at ~10-μg chlorophyll/L, the instrument as configured is well suited to make measurements in the open ocean.

The aforementioned increase in sensitivity enables single-shot spectral emission coverage through the use of a diode array instead of through an intensified diode array or photomultiplier tubes. This makes the instrument simpler, less expensive to build, and more rugged, although the disadvantage is the relatively higher level of noise introduced into the detection electronics.

When the fluorometer was deployed on the SeaSoar, a pump was used to flow seawater through the sample cell. At the flow rates used, the cell residence times were always less than 0.04 s, so that only the initial portion of the fluorescence induction curve was sampled. This results in an increase in sensitivity relative to the static sample case in that the fluorescence per cell is greater for these short residence times.

5. Summary

Use of the multiexcitation spectral fluorometer can discriminate among various species of phytoplankton on the basis of their different fluorescence efficiencies as a function of excitation wavelength. The fluorescence response of the instrument is linear as a function of extracted chlorophyll concentration from 0.1 to at least 40 μg/L, although for cultures the package effect introduces a nonlinear response at about 10 μg/L. The detection limit of the instrument is dependent on the species of phytoplankton present, their physiological state and light history, the excitation filters used in the instrument, and the number of spectra averaged. Our data show that as little as 0.1 μg chlorophyll/L could be detected in a single shot and that with averaging 100 spectra (10-s data-acquisition time) the detection limit is 0.01 μg/L. The instrument has been deployed as part of a SeaSoar instrument package on several oceanographic cruises and has worked extremely well under a range of operating conditions.

We thank Chiu Chau of Instruments, SA, for working with us to modify the SC-90 spectrometer for this application and Wim Auer of Chroma Technologies, who custom designed and shot the interference filters to our stringent specifications. We also thank Collin Roesler, now at the University of Connecticut, for help with the culture work and for the use of the Cary spectrophotometer; Scott Pegau, at Oregon State, for chlorophyll determinations with a WETLabs ac-9; and Lynne Fessenden and Alice Murphy, also at Oregon State, for growing and maintaining the cultures. This work was supported by ONR N00014-92J1535.

References

1. C. J. Lorenzen, "A method for continuous measurement of *in vivo* chlorophyll concentration," Deep-Sea Res. **13,** 223–227 (1966).
2. A. W. Herman and K. L. Denman, "Rapid underway profiling of chlorophyll with an *in situ* fluorometer mounted on a 'Batfish' vehicle," Deep-Sea Res. **24,** 385–397 (1977).
3. R. Bartz, R. W. Spinrad, and J. C. Kitchen, "A low power, high resolution, *in situ* fluorometer for profiling and moored applications in water," in *Ocean Optics IX*, M. A. Blizard, ed., Proc. SPIE **925,** 157–170 (1988).
4. Govindjee, J. Amesz, and D. C. Fork, eds., *Light Emission by Plants and Bacteria* (Academic, New York, 1986), Chaps. 16 and 17.
5. K. S. Rowan, *Photosynthetic Pigments of Algae* (Cambridge University, Cambridge, England, 1989).
6. C. S. Yentsch and C. M. Yentsch, "Fluorescence spectral signatures: the characterization of phytoplankton populations by the use of excitation and emission spectra," J. Mar. Res. **37,** 471–483 (1979).
7. C. S. Yentsch and D. A. Phinney, "Spectral fluorescence: an ataxonomic tool for studying the structure of phytoplankton populations," J. Plank. Res. **7,** 617–632 (1985).
8. W. W. Broenkow, A. J. Lewitus, and M. A. Yarbrough, "Spectral observations of pigment fluorescence in intermediate depth waters of the North Pacific," J. Mar. Res. **43,** 875–891 (1985).
9. R. Iturriaga, R. Bartz, and J. R. V. Zaneveld, "An in situ active fluorometer to measure coccoid cyanobacteria fluorescence," in *Ocean Optics X*, R. W. Spinrad, ed., Proc. SPIE **1302,** 346–354 (1990).
10. J. D. Ingle, Jr. and S. R. Crouch, *Spectrochemical Analysis* (Prentice-Hall, Englewood Cliffs, N. J., 1988).
11. J. T. O. Kirk, *Light and Photosynthesis in Aquatic Ecosystems* (Cambridge University, Cambridge, England, 1994).
12. R. A. Desiderio, T. J. Cowles, J. N. Moum, and M. Myrick, "Microstructure profiles of laser-induced chlorophyll fluorescence spectra: evaluation of backscatter and forward-scatter fiber-optic sensors," J. Atmos. Ocean. Technol. **10,** 209–224 (1993).